

## Spontaneous Solid-State Co-Crystallization of Caffeine and Urea

Pol MacFhionnghaile, Clare M. Crowley, Patrick McArdle, and Andrea Erxleben

*Cryst. Growth Des.*, **Just Accepted Manuscript** • DOI: 10.1021/acs.cgd.9b01152 • Publication Date (Web): 09 Jan 2020

Downloaded from pubs.acs.org on January 15, 2020

### Just Accepted

“Just Accepted” manuscripts have been peer-reviewed and accepted for publication. They are posted online prior to technical editing, formatting for publication and author proofing. The American Chemical Society provides “Just Accepted” as a service to the research community to expedite the dissemination of scientific material as soon as possible after acceptance. “Just Accepted” manuscripts appear in full in PDF format accompanied by an HTML abstract. “Just Accepted” manuscripts have been fully peer reviewed, but should not be considered the official version of record. They are citable by the Digital Object Identifier (DOI®). “Just Accepted” is an optional service offered to authors. Therefore, the “Just Accepted” Web site may not include all articles that will be published in the journal. After a manuscript is technically edited and formatted, it will be removed from the “Just Accepted” Web site and published as an ASAP article. Note that technical editing may introduce minor changes to the manuscript text and/or graphics which could affect content, and all legal disclaimers and ethical guidelines that apply to the journal pertain. ACS cannot be held responsible for errors or consequences arising from the use of information contained in these “Just Accepted” manuscripts.

# Spontaneous Solid-State Co-Crystallization of Caffeine and Urea

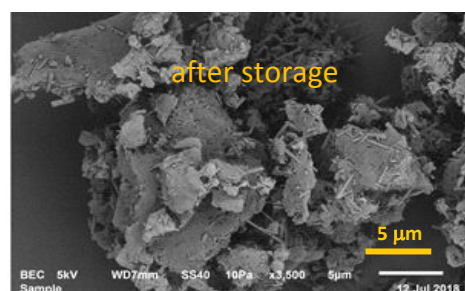
Pól MacFhionnhaile,<sup>1</sup> Clare M. Crowley,<sup>2</sup> Patrick McArdle,<sup>\*,1</sup> and Andrea Erxleben<sup>\*,1</sup>

<sup>1</sup> Synthesis and Solid State Pharmaceutical Centre and School of Chemistry, National University of Ireland Galway, Galway, H91 TK33, Ireland

<sup>2</sup> Synthesis and Solid State Pharmaceutical Centre and Department of Chemical Sciences, Bernal Institute, University of Limerick, Limerick, V94 T9PX, Ireland

## Abstract

The co-crystallization of caffeine and urea was monitored and analyzed using infrared spectroscopy, Raman microscopy, scanning electron microscopy, differential scanning calorimetry and X-ray diffraction. The caffeine-urea co-crystal was shown to form spontaneously over several weeks under low energy mixing of the solids at room temperature and low relative humidity (<30%). Pre-milling the two cofomers separately accelerated the process and the co-crystal formation could be detected within three days. When caffeine and urea were milled together, the physical mixture that was confirmed by X-ray powder diffraction immediately after milling transformed to the co-crystal within hours of storage at room temperature and 30 % relative humidity. The scanning electron microscopy images of the milled sample indicated the role of inter-particle surface contact in the spontaneous solid-state reaction. Multivariate data analysis was used to find the optimum cooling crystallization conditions for obtaining co-crystals suitable for single crystal X-ray analysis.



# Spontaneous Solid-State Co-Crystallization of Caffeine and Urea

Pól MacFhionnghaile,<sup>1</sup> Clare M. Crowley,<sup>2</sup> Patrick McArdle,<sup>\*,1</sup> and Andrea Erxleben<sup>\*,1</sup>

<sup>1</sup> Synthesis and Solid State Pharmaceutical Centre and School of Chemistry, National University of Ireland Galway, Galway, H91 TK33, Ireland

<sup>2</sup> Synthesis and Solid State Pharmaceutical Centre and Department of Chemical Sciences, Bernal Institute, University of Limerick, Limerick, V94 T9PX, Ireland

## Abstract

The co-crystallization of caffeine and urea was monitored and analyzed using infrared spectroscopy, Raman microscopy, scanning electron microscopy, differential scanning calorimetry and X-ray diffraction. The caffeine-urea co-crystal was shown to form spontaneously over several weeks under low energy mixing of the solids at room temperature and low relative humidity (<30%). Pre-milling the two cofomers separately accelerated the process and the co-crystal formation could be detected within three days. When caffeine and urea were milled together, the physical mixture that was confirmed by X-ray powder diffraction immediately after milling transformed to the co-crystal within hours of storage at room temperature and 30 % relative humidity. The scanning electron microscopy images of the milled sample indicated the role of inter-particle surface contact in the spontaneous solid-state reaction. Multivariate data analysis was used to find the optimum cooling crystallization conditions for obtaining co-crystals suitable for single crystal X-ray analysis.

## Introduction

Integrating solid-state reactions with crystallization techniques is an attractive means of adapting 'Green Chemistry' to industrial manufacturing, as one of the twelve principles of Green Chemistry is the reduction and/or possible removal of solvents from a chemical reaction.<sup>1,2</sup> Solvent-free crystallization reduces waste, cost, environmental and health impacts, as well as batch to batch variation due to solvents sourced from different suppliers with different impurity profiles. Co-crystallization allows the combination of complementary drugs e.g. the combination of drugs known to cause nausea with anti-nausea drugs, into a single crystalline phase and the optimisation of chemical, physical, and pharmacological properties.

Solid-state reactions are becoming a growing trend in organic synthesis.<sup>3</sup> They often require relatively high energy inputs *via* manual grinding (mortar and pestle),<sup>4</sup> high impact milling (mechanical rotational or oscillating milling),<sup>5</sup> or continuous grinding (twin screw extrusion, hot melt extrusion).<sup>6</sup> Recently, resonant acoustic mixing was shown to produce co-crystals under rather "soft" mixing conditions.<sup>7-10</sup> On the other hand it is known that solids with a low vapour pressure can spontaneously undergo solid-state reactions forming salts, solvates, or co-crystals.<sup>11-14</sup> Solid-state co-crystallization *via* manual grinding has been known for over a century. In 1893 Ling and Baker reacted an equimolar mixture of metadichloroquinone and metadichloroquinol to produce the metadichloroquinone-metadichloroquinol co-crystal.<sup>15</sup> Currently solid-state co-crystallization is routinely used in many fields of solid-state chemistry and pharmaceuticals.<sup>16</sup> Recent work has shown the adoption of high impact milling as a method to screen for co-crystals and co-amorphous systems.<sup>17-19</sup>

Spontaneous solid-state reactions can involve a chemical reaction or a change of the crystal structure.<sup>20,21</sup> Spontaneous solid-state reactions are well documented where surface contact with a template or another solid form induces a solid-state transformation of the material. This phenomenon is well known for mono-component systems that transform to different polymorphs.<sup>22</sup> Multi-component solid-state reactions can occur spontaneously when two different compounds come into contact and are most often observed as solvate or hydrate formation, but rarely as co-crystal formation.<sup>11-13,23</sup> If the reaction is thermodynamically and kinetically favoured, spontaneous co-crystal formation can be induced by physically mixing stoichiometric ratios of the powdered co-formers. Ibrahim *et al.* monitored the effects of humidity when mixing samples of 2-methoxybenzamide and urea, and of caffeine and

malonic acid. Humidity was shown to increase the rate of co-crystallization in both cases and a minimum level of humidity was needed to induce the reaction.<sup>14</sup> Maheshwari *et al.* used free energy calculations to predict thermodynamically favoured co-crystals of carbamazepine (carbamazepine–nicotinamide and carbamazepine–saccharin) and investigated the influence of the storage conditions on the spontaneous co-crystallization. They found that humidity and temperature play a role in co-crystal formation. A new co-crystal polymorph of carbamazepine–saccharin was produced from milled samples stored at high temperatures and humidity.<sup>23</sup> Ervasti *et al.* investigated the effects of storage conditions, starting material particle size, and the use of anhydrous theophylline or its hydrate on the formation of theophylline and nicotinamide co-crystals.<sup>12</sup> The rate of co-crystal formation increased with humidity, temperature, and particle size reduction. Using theophylline hydrate hindered the transformation to the co-crystal. Although all studies observe partial or almost complete transformation of powdered samples to the co-crystal at high temperature, no examples could be found of a system fully transforming to a co-crystal at ambient temperature and relatively low humidity.

There are several possible mechanisms for spontaneous solid-state reactions including vapour diffusion, moisture sorption, sunken eutectic-liquid phases, amorphization, solid dispersion, and long range anisotropic molecular migration.<sup>24</sup> Rastogi *et al.* and others attributed the spontaneous co-crystallization of naphthalene and picric acid to a vapour diffusion mechanism.<sup>25-29</sup> Davey and coworkers investigated the co-crystallization of benzophenone and diphenylamine and observed a submerged eutectic temperature of 13.3 °C which allowed the spontaneous reaction of two particles at room temperature.<sup>30</sup> Transient amorphous phases are well documented during grinding<sup>31-33</sup> and milling-induced co-crystallization.<sup>34</sup> Kaupp used atomic force microscopy to identify a topotactic reaction for a number of solid-state reactions.<sup>24</sup>

This work investigates the co-crystallization of caffeine and urea *via* a spontaneous solid-state reaction. Caffeine is a widely used additive in food and pharmaceuticals and has been shown to interact with urea in solution.<sup>35</sup> Urea is well known to form supramolecular assemblies. These include the urea inclusion compounds with guest molecules occupying tunnels in the urea host structure<sup>36</sup> and hydrogen-bonded co-crystals. Because of its special H bond donor and acceptor capabilities, a large number of urea co-crystals have been described, *e.g.* with carboxylic acids,<sup>37-46</sup> amides,<sup>47</sup>  $\alpha,\omega$ -dihydroxyalkanes,<sup>48-50</sup> phenols<sup>51</sup> and carbohydrates,<sup>52</sup> various of which were obtained by mechanochemical techniques. Honer *et*

1  
2  
3 *al.*, for example, reported the mechanochemical synthesis of urea ionic co-crystals with Mg  
4 and Ca salts<sup>53</sup> and Casali *et al.* prepared two polymorphs of the ionic co-crystal  
5 urea-ZnCl<sub>2</sub>-KCl by solution crystallization and mechanochemistry.<sup>54</sup> Zhou *et al.* synthesized  
6 mechanochemically polymorphs of 1:2 co-crystals of urea with 1,6-dihydroxyhexane and 1,8-  
7 dihydroxyoctane.<sup>48</sup> In the present work an in-house mixer was designed to slowly mix the  
8 physical mixture of caffeine and urea, allowing particle-particle interactions with little  
9 external energy input. Infrared spectroscopy, X-ray diffraction, Raman microscopy,  
10 differential scanning calorimetry and scanning electron microscopy were used to monitor the  
11 solid-state reaction and to characterize the co-crystal obtained. Solution crystallization  
12 experiments were carried out in order to obtain single crystals for structure determination.  
13  
14  
15  
16  
17  
18  
19  
20  
21

## 22 **Materials & Methods**

### 23 **Materials**

24 Caffeine ( $\geq 99.0\%$ ) and urea ( $\geq 98.0\%$ ) were supplied by Sigma-Aldrich (Saint Louis,  
25 Missouri, USA). Acetonitrile ( $\geq 99.9\%$ ) was purchased from Honeywell (Wabash, Indiana,  
26 USA). Diethyl ether ( $\geq 99.5\%$ ), methanol ( $\geq 99.9\%$ ), and ethyl acetate ( $\geq 99.5\%$ ) were  
27 supplied by Merck (Kenilworth, New Jersey, USA). Acetone ( $\geq 99\%$ ) and ethanol ( $\geq 99\%$ )  
28 were supplied by Fisher (Pittsburgh, Pennsylvania, USA).  
29  
30  
31  
32  
33  
34

### 35 **Methods**

#### 36 **Solid-State Analysis**

37 IR spectra were recorded using a PerkinElmer Spectrum 400 (Waltham, Massachusetts)  
38 equipped with a DATR 1 bounce Diamond/ZnSe Universal ATR sampling accessory. Spectra  
39 were measured in the range from 4000 to 650 cm<sup>-1</sup> with 8 accumulations and a resolution of  
40 4 cm<sup>-1</sup>.  
41  
42  
43  
44  
45

46 Thermal analysis was performed on a Rheometric Scientific STA625 thermal analyser  
47 (Piscataway, New Jersey) with a constant heating rate of 10 °C/min. The measurements were  
48 made in open aluminium crucibles, nitrogen was purged in ambient mode (40 mL/min) and  
49 calibration was performed using an indium standard.  
50  
51  
52

53 Raman microscopy was conducted using a Renishaw inVia confocal microscope with a  $\times 50$   
54 optical lens and the WiRE 3.4 software. Powdered samples were lightly dispersed manually  
55 on a glass slide using a spatula. Individual particles were focused and selected using a XYZ  
56  
57  
58  
59  
60

1  
2  
3 sample stage. Spectra were collected from 200 to 3200  $\text{cm}^{-1}$  using 600/cm grating (785 nm  
4 laser at 10% power; 3 acquisitions, 3 s exposure time).

7 *In-situ* SEM-Raman spectroscopy was performed on an inVIA Reflex micro-spectrometer  
8 (Renishaw, Wotton under Edge, UK) coupled to a DM2500 Leica microscope and a JSM-  
9 6510LV SEM (JEOL) equipped with secondary electron (SE (high vacuum (HV))) and  
10 backscatter electron (BSE (low vacuum (LV))) detectors. The 785 nm excitation laser  
11 (diffraction grating groove density 1800 grooves/mm) was used throughout and instrument  
12 calibration was performed using the Si (100) peak ( $520.5 \pm 1 \text{ cm}^{-1}$ ) (50 $\times$  objective, laser  
13 power 10 mW, acquisition time 10 s, 1 accumulation).

16 SEM was performed by dispersing powder samples on carbon disks (Agar, Oxford  
17 Instruments) attached to SEM stubs, placed in an SEM stub holder and a montage of the  
18 whole stub collected using the optical microscope. Following inspection of the dispersed  
19 powders on the optical microscope a region of interest was selected and spectra collected by  
20 point mapping (20 $\times$  objective, laser power 1 mW, acquisition time  $\geq 10$  s,  $\geq 5$   
21 accumulations). In the SEM the region of interest was identified using optical images of the  
22 whole stub montage and the region of interest. The particles were then examined in BSE  
23 mode (3 - 5 kV, 10 - 20 Pa) and the co-ordinates of the particles of interest and images  
24 recorded. Following focussing of the Raman laser at each point of interest the acquisition  
25 time and the number of acquisitions for each spectrum was varied to improve the signal-to-  
26 noise ratio (laser power 0.1 - 6 mW, acquisition time  $\geq 30$  secs,  $\geq 5$  accumulations), over a  
27 narrow spectral range of interest. Following spectral acquisition the samples were gold-  
28 coated (SI50B, Edwards) and the particles of interest re-examined by SEM (JSM-6510LV  
29 (JEOL)) to obtain high resolution images of the position from which spectra had been  
30 collected.

31  
32  
33  
34  
35  
36  
37  
38  
39  
40  
41  
42  
43  
44  
45  
46  
47 Single crystal X-ray diffraction was carried out on an Oxford Diffraction Xcalibur system  
48 (Oxfordshire, UK) at room temperature. The crystal structure was solved by direct methods  
49 using SHELXT and refined using SHELXL 2018/3 within the Oscale package.<sup>55-57</sup>  
50 Crystallographic data and details of refinement are reported in Table 1. The cif file can be  
51 obtained free of charge at [www.ccdc.cam.ac.uk/conts/retrieving.html](http://www.ccdc.cam.ac.uk/conts/retrieving.html) or from the Cambridge  
52 Crystallographic Data Centre, Cambridge, UK with the REF code 1935528.

53  
54  
55  
56  
57  
58  
59  
60 Powder X-ray diffraction (PXRD) patterns were collected on an Inel Equinox 3000 powder  
diffractometer (Artenay, France), fitted with a curved position sensitive detector calibrated

1  
2  
3 using  $\text{Y}_2\text{O}_3$ . Data were collected between 5 and  $90^\circ$  ( $2\theta$ ) using  $\text{Cu K}_\alpha$  radiation ( $\lambda = 1.54178$   
4  $\text{\AA}$ , 35 kV, 25 mA). Theoretical powder patterns were calculated using the Oscale software  
5 package.<sup>57</sup>  
6  
7

## 9 **Co-Crystallization**

### 11 *Milling:*

12 1 g of an equimolar mixture of caffeine and urea was milled at room temperature using an  
13 oscillating ball mill (Mixer Mill MM400; Retsch GmbH, Haan, Germany) at 25 Hz in a 25  
14 mL stainless steel jar using a 15 mm stainless steel ball. After 30 min the milling was  
15 interrupted for 15 min to avoid overheating of the sample. The milling was continued for  
16 another 30 min so that the total milling time was 60 min. The sample was stored overnight at  
17 room temperature and 30 % relative humidity (RH). The formation of the co-crystal was  
18 confirmed by PXRD.  
19  
20  
21  
22  
23  
24

25 To confirm the 1:1 interaction between the components 1:3 and 3:1 mixtures of caffeine and  
26 urea were milled at 25 Hz for 60 min (using the same procedure as above with a 15 min break  
27 after the first 30 min.), kept at room temperature for 1 d and analyzed by PXRD.  
28  
29  
30

### 31 *Mixing using an in-house low energy mixer:*

32 Caffeine and urea (1 g each) were milled separately for 60 min. with a 15 min. break after the  
33 first 30 min interval. The milled caffeine and urea were mixed in a 1:1 molar ratio (1 g in  
34 total) in a 28 mL vial (60 mm height  $\times$  20 mm diameter). The vial was attached to a bespoke  
35 low energy mixer designed to rotate at 50 rpm, 3 clockwise rotations followed by 3 counter  
36 clockwise rotations as previously described.<sup>58</sup> The mixer was assembled using an Arduino  
37 Uno R2 single board microcontroller (Ivera, Italy) to control a stepped motor spinning the  
38 vial at a *ca.*  $15^\circ$  horizontal tilt.  
39  
40  
41  
42  
43  
44

### 45 *Mixing using a magnetic stirrer:*

46 1 g of a 1:1 mixture of caffeine and urea, individually milled as described above, was placed  
47 in a 10 mL glass vial. The sample was mixed at 100 rpm using a magnetic stirring plate and a  
48  $8 \times 3$  mm stirring bar. Mixing was done at room temperature and  $<30\%$  RH.  
49  
50  
51  
52

### 53 *Crystallization from solution:*

54 Under-saturated solutions of caffeine and urea (1:1 molar ratio) were prepared in duplicate  
55 using the following solvents; methanol, ethanol, isopropanol, water, acetonitrile, and ethyl  
56 acetate. The solutions were divided into two sample sets. One sample set was seeded with the  
57  
58  
59  
60



1  
2  
3 co-crystal prepared by milling and storage, the other was allowed to crystallize unseeded.  
4 Both sample sets were left to evaporate in a fume-hood at room temperature (22 – 26 °C). IR  
5 spectra of the powders/crystals were collected and processed using Principal Component  
6 Analysis (PCA) and Unscrambler 10.1 (CAMO) to find the optimum conditions for the  
7 crystallization of the caffeine-urea cocrystal. The IR spectra were pre-treated using Standard  
8 Normal Variate (SNV) transformation on ranges containing characteristic peaks of caffeine,  
9 urea and the co-crystal and were then processed by singular value decomposition PCA with  
10 seven latent variables. Solvents from which the co-crystal crystallized after evaporation were  
11 further investigated to grow X-ray suitable single crystals by cooling crystallization.

12  
13  
14  
15  
16  
17  
18  
19 A Thermo Fisher Scientific oven (UT 6420) coupled with a Heraeus (Thermicon P)  
20 temperature controller was used for controlled cooling crystallization. A solution containing  
21 600 mg of an equimolar caffeine and urea mixture in 15 mL of acetonitrile was held at 70 °C  
22 for 12 h, then cooled to 25 °C with temperature cycling over the course of several days.  
23  
24  
25  
26  
27  
28  
29

## 30 Results

### 31 Caffeine-Urea Co-crystal Formation in Milled Samples

32 An equimolar mixture of caffeine and urea was milled for 60 min. and the milled sample was  
33 analyzed by PXRD and IR spectroscopy (Figure 1). Immediately after milling peaks in the  
34 PXRD pattern match the peaks of commercial urea and caffeine, indicating that no new  
35 crystalline material was formed. Although there are no changes in peak position, changes in  
36 intensity are observed. The peaks of caffeine are slightly reduced, whereas all peaks  
37 associated with urea are reduced by a factor of five (Figure S1, SI). It is unlikely that  
38 preferred orientation effects are the reason for the intensity decrease, as preferred orientation  
39 would only affect certain peaks and not all. The loss of intensity is likely caused by a  
40 reduction in particle size and crystallinity during milling.<sup>59</sup> Although no new crystalline  
41 material was detected immediately after milling, when the milled sample was stored at room  
42 temperature new peaks were observed at 8.64°, 10.82°, 13.89°, 24.30°, 25.08°, 25.46°, and  
43 28.07° ( $2\theta$ ) in the PXRD pattern. This new pattern was compared to the calculated patterns of  
44 the urea and caffeine structures reported in the CSD (Figure S2, SI) ruling out a simple  
45 polymorphic transformation. Instead the new peaks can be attributed to a spontaneous co-  
46 crystal formation during storage as confirmed by comparing the experimental PXRD pattern  
47 with the simulated PXRD pattern calculated from the single crystal data of the urea-caffeine  
48  
49  
50  
51  
52  
53  
54  
55  
56  
57  
58  
59  
60

1  
2  
3 co-crystal obtained by solution crystallization (see below). Figure 2 shows the change in the  
4 normalized peak heights of the caffeine peaks at 11.7 and 26.5° ( $2\theta$ ) and of the urea peak at  
5 22.7° ( $2\theta$ ) vs. storage time.  
6  
7

8  
9 The solid-state transformation during storage of milled caffeine and urea was also monitored  
10 using IR spectroscopy. Figure 1a shows the calculated spectrum of an equimolar physical  
11 mixture of caffeine and urea overlaid with the spectrum of caffeine and urea immediately  
12 after milling. Immediately after milling slight changes in the IR spectrum are seen. Most  
13 notably the caffeine  $\nu(\text{C}=\text{O})$  band at 1677  $\text{cm}^{-1}$  is shifted to 1682  $\text{cm}^{-1}$  and the urea  $\nu_{\text{s}}(\text{N}-\text{H})$   
14 band is shifted from 3341  $\text{cm}^{-1}$  to 3335  $\text{cm}^{-1}$  with a new shoulder at 3347  $\text{cm}^{-1}$ . When the  
15 milled sample is stored overnight at room temperature more significant changes are observed  
16 indicating changes in H-bonding interactions and the formation of the co-crystal. The  
17 caffeine  $\nu(\text{C}=\text{O})$  peak at 1682  $\text{cm}^{-1}$  is shifted to 1707  $\text{cm}^{-1}$  and the  $\nu_{\text{s}}(\text{N}-\text{H})$  urea peak is  
18 shifted to 3185  $\text{cm}^{-1}$ . Similar, large shifts of  $\sim 200 \text{ cm}^{-1}$  were reported for the  $\nu_{\text{s}}(\text{N}-\text{H})$  band in  
19 other urea co-crystals.<sup>60</sup> The spectrum also shows the convolution of several peaks  
20 throughout the spectrum and the appearance of a new peak at 809  $\text{cm}^{-1}$  unique to the co-  
21 crystal. The discrepancy between the IR and PXRD data of the samples analyzed directly  
22 after milling may be due to the fact that ATR-FTIR spectroscopy is a surface-biased  
23 technique. A Diamond/ ZnSe ATR-IR has a penetration depth of 1.66  $\mu\text{m}$ , resulting in an  
24 overemphasis of changes on the particle surface.  
25  
26  
27  
28  
29  
30  
31  
32  
33  
34  
35  
36

37 To investigate the co-crystallization of caffeine and urea further, mixtures of different  
38 stoichiometric ratios, 1:3 and 3:1, were milled for 60 min. and analyzed 24 h after preparation  
39 (Figure S3, SI). The PXRD patterns and IR spectra of both ratios show mixtures of the co-  
40 crystal and excess starting material. This indicates a 1:1 interaction between caffeine and urea  
41 with no other transformation taking place.  
42  
43  
44  
45  
46  
47  
48

### 49 **Mixing of Caffeine and Urea Using a Low Energy Mixer**

50 Caffeine and urea were milled separately for 60 min. at 25 Hz. No solid-state changes were  
51 observed after milling by IR spectroscopy or PXRD. The milled caffeine and urea were then  
52 mixed in a 1:1 molar ratio in an in-house low energy mixer<sup>58</sup> at room temperature and <30 %  
53 relative humidity. Direct transformation of the caffeine and urea physical mixture to the co-  
54 crystal was observed and monitored using IR spectroscopy (Figure 3). Transformation was  
55 detected within three days. Peaks specific to the co-crystal (1707 and 809  $\text{cm}^{-1}$ ) as well as the  
56  
57  
58  
59  
60

1  
2  
3 characteristic shift of the  $\nu_s(\text{N-H})$  urea band to  $3185\text{ cm}^{-1}$  were observed. At the same time  
4 the caffeine and urea bands at  $1677$  and  $3341\text{ cm}^{-1}$  decreased in intensity. By contrast, when  
5 an equimolar mixture of un-milled caffeine and urea was mixed using the low energy mixer,  
6 a small broad peak at  $809\text{ cm}^{-1}$  in the IR spectrum indicated the formation of only a small  
7 amount of the caffeine-urea co-crystal after 10 weeks (Figure S4, SI).  
8  
9

10  
11  
12 More aggressive mixing of unmilled caffeine-urea using a magnetic stirrer increased the rate  
13 of transformation to the co-crystal when compared to the low energy mixing. IR and PXRD  
14 peaks characteristic to the co-crystal appeared within five weeks (Figure S5).  
15  
16

17  
18 Equimolar physical mixtures of separately milled caffeine and urea and of un-milled caffeine  
19 and urea were left without mixing as controls for two months. No changes were observed in  
20 the IR spectra or PXRD patterns.  
21  
22  
23  
24  
25

## 26 27 **DSC Analysis**

28  
29 Figure 4 compares the DSC thermograms of an equimolar physical mixture of caffeine and  
30 urea before milling, immediately after milling for 60 min. and after storing the milled sample  
31 for 24 h. Immediately after milling the caffeine-urea sample shows an exotherm at  $91.3\text{ }^\circ\text{C}$   
32 and a sharp endotherm at  $132.7\text{ }^\circ\text{C}$ , slightly lower than the melting point of urea ( $135.3\text{ }^\circ\text{C}$ ).  
33 The former indicates the transformation into the co-crystal and the latter is assigned to the  
34 melting of the co-crystal. A melting endotherm at  $132.7\text{ }^\circ\text{C}$  is also observed in the  
35 thermogram of the caffeine-urea co-crystal prepared by cooling crystallization from  
36 acetonitrile (see below). After storing the milled sample for 24 h at room temperature the  
37 exotherm at  $91.3\text{ }^\circ\text{C}$  is no longer observed. This corroborates that the exotherm at  $91.3\text{ }^\circ\text{C}$  is  
38 due to the transformation of the caffeine-urea sample (still present as a physical mixture  
39 directly after milling) to the co-crystal. This transformation is not seen in the DSC plot of the  
40 un-milled physical mixture and this is due to the lack of contact between caffeine and urea  
41 particles in this sample (see SEM images discussed below).  
42  
43  
44  
45  
46  
47  
48  
49  
50  
51  
52  
53

## 54 55 **Crystal Growth and Single Crystal X-ray Structure**

56 Various solvents were investigated in order to obtain single crystals of the caffeine-urea co-  
57 crystal; methanol (MeOH), ethanol (EtOH), water, acetone (Ace), acetonitrile (Atrn), ethyl  
58 acetate (EtA), and isopropanol (IPA). Undersaturated solutions of caffeine and urea (1:1)  
59  
60

1  
2  
3 were prepared in duplicate. One sample set was left to evaporate unseeded using each solvent  
4 (xxxx\_U, where xxxx is the solvent and U indicates the sample was unseeded). The other  
5 sample set was seeded using the co-crystal prepared by milling and left to slowly evaporate at  
6 room temperature (xxxx\_S, with S indicating seeding).  
7  
8  
9

10  
11 Figure 5 shows the 3D PCA scores plot explaining 95 % of the information of the 3650 –  
12 2825 cm<sup>-1</sup>, 1755 – 1325 cm<sup>-1</sup>, and 940 – 750 cm<sup>-1</sup> ranges of the SNV pre-processed IR spectra  
13 of the evaporated samples. Caffeine, urea, and the co-crystal are well separated, with most  
14 solvents (seeded and unseeded) giving mixtures of the starting materials and the co-crystal.  
15 From unseeded acetone solutions only the co-crystal crystallized, while seeding gave  
16 mixtures of the co-crystal, urea and caffeine which crystallized in different regions of the  
17 evaporation dish. Both seeded and unseeded crystallization from acetonitrile gave the pure  
18 co-crystal. Hence acetonitrile was chosen as the solvent to produce single crystals for X-ray  
19 analysis *via* cooling crystallization.  
20  
21  
22  
23  
24  
25

26  
27 Initial samples from cooling crystallization using acetonitrile produced thin, aggregated  
28 needles unsuitable for single crystal XRD. Because of this a slower cooling rate was used  
29 with temperature cycling at critical points of crystal growth where aggregation/agglomeration  
30 was expected. Cooling from 70 °C to 25 °C at a rate of ~0.3 °C h<sup>-1</sup>, with an increase of 1 °C  
31 followed by a decrease of 2 °C between 60 and 55 °C enabled crystal growth to the size and  
32 quality where single crystal XRD was feasible.  
33  
34  
35  
36

37  
38 The caffeine-urea cocrystals grew as needles extended along the *c* axis (Figure S6). In the  
39 crystal structure the caffeine molecules were disordered over two positions with 75 and 25 %  
40 occupancies. The principal component of the disorder is shown in Figure 6. The hydrogen  
41 bonding scheme has hydrogen bonded urea ladders running parallel to the *c* axis with the  
42 caffeine molecules hydrogen bonded to these chains, Figures 6b and 6c and Table S1.  
43 Adjacent chains along *b* have the hydrogen bonded caffeine molecules alternating in the vdW  
44 contact stacks along *c*. The crystal structure is well packed with a 69 % packing coefficient  
45 and the caffeine molecule stacking along *c* has 80 % of the atoms in each molecule in vdW  
46 contact with their stack neighbours. This vdW contact stacking is probably the reason for the  
47 needle growth along *c*.<sup>61</sup> Figure S7 compares the experimental PXRD patterns of the co-  
48 crystals formed spontaneously during storage of the milled mixture, the co-crystal isolated  
49 from solution and the theoretical pattern calculated from the single crystal data. All peaks  
50 align within 0.25° (*2θ*). The PXRD pattern of the sample crystallized from solution shows  
51  
52  
53  
54  
55  
56  
57  
58  
59  
60

1  
2  
3 preferred orientation effects. It would be interesting to see whether the co-crystals that were  
4 obtained by solid-state transformation of milled or low-energy mixed samples have the same  
5 disorder as the crystals formed in solution. However, the calculated PXRD patterns for the  
6 major and the minor component of the single-crystal structure are identical without any  
7 significant differences in the relative intensities (Figure S8) so that the experimental  
8 diffractograms of the mechanochemically prepared samples cannot give further insight into  
9 their disorder.  
10  
11  
12  
13  
14  
15  
16  
17

### 18 **Raman Microscopy and SEM**

19  
20 Raman microscopy was performed on multiple regions of several crystals obtained by milling  
21 and storage. The spectra were compared with those of caffeine, urea, and the co-crystal  
22 produced by cooling crystallization (Figure 7). Raman spectra taken throughout the length of  
23 multiple crystals of the co-crystal have consistently peaks specific to the co-crystal at 1710.8,  
24 505.3, and 108.6  $\text{cm}^{-1}$ .  
25  
26  
27  
28

29 SEM micrographs of the as-received and milled urea and caffeine samples confirmed that  
30 milling results in a reduction in the primary particle size as shown in Figure 8 (additional  
31 micrographs are included in the Supporting Information, Figure S9). Before milling the urea  
32 particles show no distinct particulate features and vary in the length of their longest axis  
33 between 200 and 800  $\mu\text{m}$ , whereas particles of milled urea show a rough corrugated surface  
34 and are agglomerated particles of approximately 2  $\mu\text{m}$ . The reduction in the primary particle  
35 size of the milled urea may explain why PXRD indicates a reduction in the relative  
36 crystallinity of the milled urea whereas no significant differences are observed in the IR  
37 spectra before and after milling. A comparison of the micrographs of unmilled and milled  
38 caffeine shows that the aggregated needle like caffeine particles of 5 – 30  $\mu\text{m}$  size (Figure 8c)  
39 break up into aggregates of about half the size with thinner needles with higher aspect ratios  
40 (Figure 8d).  
41  
42  
43  
44  
45  
46  
47  
48  
49

50 SEM micrographs of the freshly milled caffeine and urea mixture (1:1) and of the mixture  
51 stored for one week allowing the transformation to the co-crystal are compared in Figures 8e  
52 and 8f. Immediately after milling the SEM images show larger particles (urea) engrained and  
53 covered by smaller and finer crystals (caffeine). These samples transformed to the co-crystal  
54 within hours. Aged samples had converted to needles of a fairly uniform size with a length of  
55 approximately 2  $\mu\text{m}$  and an aspect ratio intermediary of that of the particles of the unmilled  
56  
57  
58  
59  
60

1  
2  
3 and milled caffeine samples. It is proposed that the spontaneous co-crystal formation in the  
4 milled sample is due to surface effects induced by milling, as milled samples show direct  
5 contact of smaller caffeine particles spread over the surface of urea particles. By contrast, the  
6 SEM images of caffeine and urea milled separately and mixed using the low energy mixer  
7 revealed aggregates of caffeine needles assembled onto urea (Figure S10).  
8  
9  
10  
11  
12  
13  
14

### 15 **Effects of Surface Contact on Co-Crystallization**

16 As described in the introduction, various mechanisms have been proposed for solid-state co-  
17 crystallization. One of the mechanisms proposed for the spontaneous transformation of a  
18 physical mixture to a co-crystal is vapour diffusion of the two solids. However, this seems  
19 unlikely in this case. Caffeine and urea have vapour pressures of  $9.0 \times 10^{-7}$  mm Hg and  $1.2 \times$   
20  $10^{-5}$  mm Hg respectively,<sup>62,63</sup> while in most spontaneous solid-state reactions that take place  
21 *via* vapour diffusion at least one solid has a vapour pressure in the  $10^{-1}$  -  $10^{-4}$  mm Hg range. A  
22 eutectic melt-mediated mechanism can also be excluded, as the thermal analysis of a physical  
23 caffeine-urea mixture did not show any endothermic event below 132.7 °C. Grinding-induced  
24 defects and lattice distortions, *i.e.* mechanical activation, can play a role in milling-mediated  
25 solid-state transformations.<sup>64</sup> Mechanical activation by milling the two components  
26 individually was also described for carbamazepine co-crystals with nicotinamide and  
27 saccharin.<sup>23</sup> In addition, surface contact seems to be an important factor here as the effect on  
28 the rate of spontaneous co-crystallization is most prominent when caffeine and urea are  
29 milled together. These samples undergo the fastest transformation to the co-crystal on storage  
30 and the co-crystal formation can be observed in the DSC plot as an exothermic event at 91.3  
31 °C. As seen in the SEM images immediately after milling, caffeine-urea samples contain  
32 small particles of caffeine ingrained onto urea particles giving tight particle-particle contact.  
33 Conversely, the transformation is slowest, when (un-milled) urea and caffeine are subjected  
34 to low energy mixing. This mixture has the largest particles and the least particle-particle  
35 surface contact. When caffeine and urea are pre-milled separately, the transformation rate  
36 under low energy mixing is increased compared to the un-milled physical mixture, as the  
37 larger surface-to-volume ratio leads to enhanced particle-particle surface contact during  
38 mixing. These observations are in agreement with the work by Ibrahim *et al.* who showed  
39 that the rate of spontaneous formation of the caffeine-malonic acid and urea-2-  
40 methoxybenzamide co-crystals during low-energy convection mixing increased with  
41  
42  
43  
44  
45  
46  
47  
48  
49  
50  
51  
52  
53  
54  
55  
56  
57  
58  
59  
60

1  
2  
3 decreasing particle size of the pre-milled components.<sup>14</sup> It was proposed that inter-particle  
4 contact and increase in contact areas are the main factors in the accelerated spontaneous co-  
5 crystal formation. In our case the different co-crystallization kinetics suggest that while the  
6 particle size matters in the spontaneous co-crystallization of caffeine and urea, tight particle-  
7 particle contact is more important in this system.  
8  
9  
10  
11  
12

## 13 14 15 Conclusions

16  
17 The formation of the 1:1 co-crystal of caffeine and urea readily occurs in the solid state. Little  
18 energy input is needed to transform a physical mixture of the two components to the co-  
19 crystal at room temperature and <30% RH. Milling caffeine and urea together greatly  
20 increases the rate of co-crystallization during storage and this can be attributed to enhanced  
21 inter-particle surface contact.  
22  
23  
24  
25  
26  
27  
28

## 29 Acknowledgements

30  
31 This publication has emanated from research supported in part by a research grant from  
32 Science Foundation Ireland (SFI) and is co-funded under the European Regional  
33 Development Fund under Grant Number 12/RC/2275. We thank Mr Ciaran O'Malley for  
34 assisting with the collection of SEM images.  
35  
36  
37  
38  
39  
40  
41

## 42 Supporting Information

43  
44 Hydrogen bonding interactions, additional XRPD patterns, IR spectra and SEM images.  
45  
46  
47

## 48 References

- 49  
50 (1) Cue, B. W.; Zhang, J. Green process chemistry in the pharmaceutical industry. *Green*  
51 *Chem. Lett. Rev.* **2009**, 2, 193– 211.  
52  
53 (2) Anastas, P. T.; Warner, J. C. *Green Chemistry: Theory and Practice*. ed.; Oxford  
54 University Press Oxford: 2000; Vol. 30.  
55  
56  
57  
58  
59  
60

- 1  
2  
3 (3) Kaupp, G. Organic Solid-State Reactions. *Encyclopedia of Physical Organic Chemistry*  
4 **2016**, 1–80.  
5  
6  
7 (4) Cheung, E. Y.; Kitchin, S. J.; Harris, K. D. M.; Imai, Y.; Tajima, N.; Kuroda, R. Direct  
8 Structure Determination of a Multicomponent Molecular Crystal Prepared by a Solid-State  
9 Grinding Procedure. *J. Am. Chem. Soc.* **2003**, *125*, 14658–14659.  
10  
11  
12 (5) Jones, W.; Eddleston, M. D. Introductory Lecture: Mechanochemistry, a versatile  
13 synthesis strategy for new materials. *Faraday Discuss.* **2014**, *170*, 9– 34.  
14  
15  
16 (6) Crawford, D. E.; Casaban, J. Recent Developments in Mechanochemical Materials  
17 Synthesis by Extrusion. *Adv. Mater.* **2016**, *28*, 5747–5754.  
18  
19  
20 (7) Michalchuk, A. A. L.; Hope, K. S.; Kennedy, S. R.; Blanco, M. V.; Boldyreva, E. V.;  
21 Pulham, C. R. Ball-free mechanochemistry: in situ real-time monitoring of pharmaceutical  
22 co-crystal formation by resonant acoustic mixing. *Chem. Commun.* **2018**, *54*, 4033– 4036.  
23  
24  
25 (8) Anderson, S. R.; Am Ende, D. J.; Salan, J. S.; Samuels, P. Preparation of an  
26 Energetic-Energetic Cocrystal using Resonant Acoustic Mixing. *Propellants, Explos.,*  
27 *Pyrotech.* **2014**, *39*, 637–640.  
28  
29  
30 (9) Am Ende, D. J.; Anderson, S. R.; Salan, J. S. Development and Scale-Up of Cocrystals  
31 Using Resonant Acoustic Mixing. *Org. Process Res. Dev.* **2014**, *18*, 331–341.  
32  
33  
34 (10) Nagapudi, K.; Umanzor, E. Y.; Masui, C. High-throughput screening and scale-up of  
35 cocrystals using resonant acoustic mixing. *Int. J. Pharm.* **2017**, *521*, 337–345.  
36  
37  
38 (11) Sarcevic, I.; Orola, L.; Belyakov, S.; Veidis, M. V. Spontaneous cocrystal hydrate  
39 formation in the solid state: crystal structure aspects and kinetics. *New J. Chem.* **2013**, *37*,  
40 2978–2982.  
41  
42  
43 (12) Ervasti, T.; Aaltonen, J.; Ketolainen, J. Theophylline–nicotinamide cocrystal formation  
44 in physical mixture during storage. *Int. J. Pharm.* **2015**, *486*, 121–130.  
45  
46  
47 (13) Arora, K. K.; Tayade, N. G.; Suryanarayanan, R. Unintended Water Mediated Cocrystal  
48 Formation in Carbamazepine and Aspirin Tablets. *Mol. Pharm.* **2011**, *8*, 982–989.  
49  
50  
51 (14) Ibrahim, A. Y.; Forbes, R. T.; Blagden, N. Spontaneous crystal growth of co-crystals:  
52 the contribution of particle size reduction and convection mixing of the co-formers.  
53 *CrystEngComm* **2011**, *13*, 1141–1152.  
54  
55  
56  
57  
58  
59  
60



- 1  
2  
3 (15) Ling, A. R.; Baker, J. L. XCVI.—Halogen derivatives of quinone. Part III. Derivatives  
4 of quinhydrone. *J. Chem. Soc., Trans.* **1893**, *63*, 1314–1327.  
5  
6  
7 (16) Kavanagh, O. N.; Croker, D. M.; Walker, G. M.; Zaworotko, M. J. Pharmaceutical  
8 Cocrystals: from Serendipity to Design to Application. *Drug Discov. Today* **2019**, *24*, 796–  
9 804.  
10  
11  
12 (17) Kasten, G.; Grohganz, H.; Rades, T.; Lobmann, K. Development of a screening method  
13 for co-amorphous formulations of drugs and amino acids. *Eur. J. Pharm. Sci.* **2016**, *95*, 28–  
14 35.  
15  
16  
17 (18) Walker, G.; Römann, P.; Poller, B.; Löbmann, K.; Grohganz, H.; Rooney, J. S.; Huff, G.  
18 S.; Smith, G. P. S.; Rades, T.; Gordon, K. C.; Strachan, C. J.; Fraser-Miller, S. J. Probing  
19 Pharmaceutical Mixtures during Milling: The Potency of Low-Frequency Raman  
20 Spectroscopy in Identifying Disorder. *Mol. Pharm.* **2017**, *14*, 4675–4684.  
21  
22  
23 (19) Gniado, K.; MacFhionnghaile, P.; McArdle, P.; Erxleben, A. The natural bile acid  
24 surfactant sodium taurocholate (NaTC) as a cofomer in coamorphous systems: Enhanced  
25 physical stability and dissolution behavior of coamorphous drug-NaTc systems. *Int. J.*  
26 *Pharm.* **2018**, *535*, 132–139.  
27  
28  
29 (20) Vittal, J. J.; Quah, H. S. Engineering solid state structural transformations of metal  
30 complexes. *Coord. Chem. Rev.* **2017**, *342*, 1–18.  
31  
32  
33 (21) Byrn, S. R.; Pfeiffer, R. R.; Stephenson, G.; Grant, D. J. W.; Gleason, W. B. Solid-State  
34 Pharmaceutical Chemistry. *Chem. Mater.* **1994**, *6*, 1148–1158.  
35  
36  
37 (22) Bučar, D.-K.; Lancaster, R. W.; Bernstein, J. Disappearing Polymorphs Revisited.  
38 *Angew. Chem. Int. Ed.* **2015**, *54*, 6972–6993.  
39  
40  
41 (23) Maheshwari, C.; Jayasankar, A.; Khan, N. A.; Amidon, G. E.; Rodríguez-Hornedo, N.  
42 Factors that influence the spontaneous formation of pharmaceutical cocrystals by simply  
43 mixing solid reactants. *CrystEngComm* **2009**, *11*, 493–500.  
44  
45  
46 (24) Kaupp, G. Solid-state molecular syntheses: complete reactions without auxiliaries based  
47 on the new solid-state mechanism. *CrystEngComm* **2003**, *5*, 117–133.  
48  
49  
50 (25) Rastogi, R. P.; Bassi, P. S.; Chadha, S. L. Kinetics of reaction between naphthalene and  
51 picric acid in the solid state. *J. Phys. Chem.* **1962**, *66*, 2707–2708.  
52  
53  
54  
55  
56  
57  
58  
59  
60

- 1  
2  
3 (26) Rastogi, R. P.; Singh, N. B.; Singh, N. B. Chemistry of organic eutectics: II. The  
4 naphthalene-p-chloronitrobenzene eutectic system. *J. Cryst. Growth* **1977**, *37*, 329–333.  
5  
6  
7 (27) Ross, S. D.; Kuntz, I. Molecular Compounds. II. Picric Acid-Naphthalene, Picric Acid-  
8 m-Dinitrobenzene and Picric Acid-1,3,5-Trinitrobenzene in Chloroform. *J. Am. Chem. Soc.*  
9 **1954**, *76*, 74–76.  
10  
11  
12  
13 (28) Rastogi, R. P.; Bassi, P. S.; Chadha, S. L. Mechanism of the reaction between  
14 hydrocarbons and picric acid in the solid state. *J. Phys. Chem.* **1963**, *67*, 2569–2573.  
15  
16  
17 (29) Banerjee, A.; Brown, C. J. Picric acid-naphthalene 1/1 [pi] complex, C<sub>6</sub>H<sub>3</sub>N<sub>3</sub>O<sub>7</sub>·C<sub>10</sub>H<sub>8</sub>. A  
18 disordered structure. *Acta Crystallogr. C* **1985**, *41*, 82–84.  
19  
20  
21 (30) Chadwick, K.; Davey, R.; Cross, W. How does grinding produce co-crystals? Insights  
22 from the case of benzophenone and diphenylamine. *CrystEngComm* **2007**, *9*, 732–734.  
23  
24  
25 (31) MacFhionnngaile, P.; Hu, Y.; Gniado, K.; Curran, S.; McArdle, P.; Erxleben, A. Effects  
26 of Ball-Milling and Cryomilling on Sulfamerazine Polymorphs: A Quantitative Study. *J.*  
27 *Pharm. Sci.* **2014**, *103*, 1766–1778.  
28  
29  
30  
31 (32) Hu, Y.; MacFhionnngaile, P.; Caron, V.; Tajber, L.; Healy, A. M.; Erxleben, A.;  
32 McArdle, P. Formation, Physical Stability, and Quantification of Process-Induced Disorder in  
33 Cryomilled Samples of a Model Polymorphic Drug. *J. Pharm. Sci.* **2013**, *102*, 93–103.  
34  
35  
36  
37 (33) Caron, V.; Hu, Y.; Tajber, L.; Erxleben, A.; Corrigan, O. I.; McArdle, P.; Healy, A. M.  
38 Amorphous solid dispersions of sulfonamide/soluplus® and sulfonamide/PVP prepared by  
39 ball milling. *AAPS PharmSciTech* **2013**, *14*, 464–474.  
40  
41  
42  
43 (34) Healy, A. M.; Worku, Z. A.; Kumar, D.; Madi, A. M. Pharmaceutical solvates, hydrates  
44 and amorphous forms: A special emphasis on cocrystals. *Adv. Drug Deliv. Rev.* **2017**, *117*,  
45 25–46.  
46  
47  
48  
49 (35) Tavagnacco, L.; Schnupf, U.; Mason, P. E.; Saboungi, M.-L.; Cesàro, A.; Brady, J. W.  
50 Molecular Dynamics Simulation Studies of Caffeine Aggregation in Aqueous Solution. *J.*  
51 *Phys. Chem. B* **2011**, *115*, 10957–10966.  
52  
53  
54  
55 (36) Harris, K. D. M. Meldola Lecture: understanding the properties of urea and thiourea  
56 inclusion compounds. *Chem. Soc. Rev.* **1997**, *26*, 279–289.  
57  
58  
59  
60

- 1  
2  
3  
4 (37) Jyothi, K. L.; Gautam, R.; Swain, D.; Guru Row, T. N.; Lokanath, N. K. Cocrystals of  
5 gallic acid with urea and propionamide: supramolecular structures, Hirshfeld surface analysis,  
6 and DFT studies. *Cryst. Res. Technol.* **2019**, *54*, 1900016.  
7  
8  
9 (38) Harkema, S.; ter Brake, J. H. M.; Helmholdt, R. B. Structure of urea-oxalic acid (1/1),  
10  $\text{CH}_4\text{N}_2\text{O} \cdot \text{C}_2\text{H}_2\text{O}_4$ , determined by neutron diffraction. *Acta Crystallogr. C* **1984**, *40*, 1733–  
11 1734.  
12  
13  
14 (39) Colman, P. M.; Medlin, E. H. The crystal structure of urea parabanic acid. *Acta*  
15 *Crystallogr. B* **1970**, *26*, 1547– 1553.  
16  
17  
18 (40) Emsley, J.; Reza, N. M.; Kuroda, R. J. Hydrogen bonding of urea-salicylic acid, U-SA.  
19 *Crystallogr. Spectrosc. Res.* **1986**, *16*, 57–69.  
20  
21  
22 (41) Videnova Adrabinska, V.; Etter, M. C. J. Urea-glutaric acid (2:1) structural aggregates  
23 as building blocks for crystal engineering. *Chem. Crystallogr.* **1995**, *25*, 823–829.  
24  
25  
26 (42) Smith, G.; Baldry, K. E.; Byriel, K. A.; Kennard, C. H. L. Molecular cocrystals of  
27 carboxylic acids. XXV The utility of urea in structure making with carboxylic acids and the  
28 crystal structures of a set of six adducts with aromatic acids. *Aust. J. Chem.* **1997**, *50*, 727–  
29 736.  
30  
31  
32 (43) Smith, G.; Kennard, C. H. L.; Byriel, K. A. The preparation and crystal structures of a  
33 series of urea adducts: with fumaric acid (2 : 1), with itaconic scid (1 : 1) and with cyanuric  
34 acid (1 : 1). *Aust. J. Chem.* **1997**, *50*, 1021–1025.  
35  
36  
37 (44) Smith, G.; Baldry, K. E.; Kennard, C. H. L.; Byriel, K. A. The preparation and crystal  
38 structure of the 1 : 1 adduct of glycine with urea. *Aust. J. Chem.* **1997**, *50*, 737–739.  
39  
40  
41 (45) Cruz-Cabeza, A. J.; Day, G. M.; Jones, W. Towards prediction of stoichiometry in  
42 crystalline multicomponent complexes. *Chem.—Eur. J.* **2008**, *14*, 8830–8836.  
43  
44  
45 (46) Chadwick, K.; Davey, R.; Sadiq, G.; Cross, W.; Pritchard, R. The utility of a ternary  
46 phase diagram in the discovery of new co-crystal forms. *CrystEngComm* **2009**, *11*, 412–414.  
47  
48  
49 (47) Cysewski, P.; Przybyłek, M.; Ziolkowska, D.; Mrocynska, K. Exploring the  
50 cocrystallization potential of urea and benzamide. *J. Mol. Model* **2016**, *22*, 103–103.  
51  
52  
53  
54  
55  
56  
57  
58  
59  
60

- 1  
2  
3 (48) Zhou, Y.; Guo, F.; Hughes, C. E.; Browne, D. L.; Peskett, T. R.; Harris, K. D. M.  
4 Discovery of new metastable polymorphs in a family of urea co-crystals by solid-state  
5 mechanochemistry. *Cryst. Growth Des.* **2015**, *15*, 2901–2907.  
6  
7  
8  
9 (49) Lee, S.-O.; Harris, K. D. M.; Kariuki, B. M. Hydrogen-bonded chains of  $\alpha,\omega$ -  
10 diaminoalkane and  $\alpha,\omega$ -dihydroxyalkane guest molecules lead to disrupted tunnel structures  
11 in urea inclusion compounds. *New J. Chem.* **2005**, *29*, 1266–1271.  
12  
13  
14 (50) Martí-Rujas, J.; Kariuki, B. M.; Hughes, C. E.; Morte-Ródenas, A.; Guo, F.; Glavcheva-  
15 Laleva, Z.; Taştēmür, K.; Ooi, L.-L.; Yeo, L.; Harris, K. D. M. Structural diversity, but no  
16 polymorphism, in a homologous family of co-crystals of urea and  $\alpha,\omega$ -dihydroxyalkanes.  
17 *New J. Chem.* **2011**, *35*, 1515–1521.  
18  
19  
20 (51) Pickering, M.; Small, R. W. H. Structure of the 1:1 complex of resorcinol and urea. *Acta*  
21 *Crystallogr. B* **1982**, *38*, 3161–3163.  
22  
23  
24 (52) Snyder, R. L.; Rosenstein, R. D. The crystal and molecular structure of the 1:1 hydrogen  
25 bond complex between [ $\alpha$ ]-D-glucose and urea. *Acta Crystallogr. B* **1971**, *27*, 1969–  
26 1975.  
27  
28  
29 (53) Honer, K.; Pico, C.; Baltrusaitis, J. Reactive mechanosynthesis of urea ionic cocrystal  
30 fertilizer materials from abundant low solubility magnesium- and calcium-containing  
31 minerals. *ACS Sustainable Chem. Eng.* **2018**, *6*, 4680–4687.  
32  
33  
34 (54) Casali, L.; Mazzei, L.; Shemchuk, O.; Honer, K.; Grepioni, F.; Ciurli, S.; Braga, D.;  
35 Baltrusaitis, J. Smart urea ionic co-crystals with enhanced urease inhibition activity for  
36 improved nitrogen cycle management. *Chem. Commun.* **2018**, *54*, 7637–7640.  
37  
38  
39 (55) Sheldrick, G. M. SHELXT - Integrated space-group and crystal-structure determination.  
40 *Acta Cryst.* **2015**, *A71*, 3–8.  
41  
42  
43 (56) Sheldrick, G. M. Crystal structure refinement with SHELXL. *Acta Cryst.* **2015**, *C71*, 3–  
44 8.  
45  
46  
47 (57) McArdle, P. Oscale, a program package for small-molecule single-crystal  
48 crystallography with crystal morphology prediction and molecular modelling. *J. Appl.*  
49 *Crystallogr.* **2017**, *50*, 320–326.  
50  
51  
52 (58) Civati, F.; Erxleben, A.; Kellehan, S.; McArdle, P. Conversion of gel-forming crystal  
53 needles to easily processable more equant crystals using high-shear-ultra-low-attrition  
54  
55  
56  
57  
58  
59  
60

1  
2  
3 agitation: Accelerated Ostwald ripening without crystal attrition. *Cryst. Growth Des.* **2019**,  
4 *19*, 1502–1504.

5  
6  
7 (59) Chikhalia, V.; Forbes, R. T.; Storey, R. A.; Ticehurst, M. The effect of crystal  
8 morphology and mill type on milling induced crystal disorder. *Eur. J. Pharm. Sci.* **2006**, *27*,  
9 19–26.

10  
11  
12 (60) Tothadi, S. Polymorphism in cocrystals of urea:4,4'-bipyridine and salicylic acid:4,4'-  
13 bipyridine. *CrystEngComm* **2014**, *16*, 7587–7597.

14  
15  
16 (61) Walshe, N.; Crushell, M.; Karpinska, J.; Erxleben, A.; McArdle, P. Anisotropic crystal  
17 growth in flat and non-flat systems: The important influence of vdW contact molecular  
18 stacking on crystal growth and dissolution. *Cryst. Growth Des.*, **2015**, *15*, 3235–3248.

19  
20  
21 (62) Jones, A. H. Sublimation Pressure Data for Organic Compounds. *J. Chem. Eng. Data*  
22 **1960**, *5*, 196–200.

23  
24  
25 (63) Emel'yanenko, V. N.; Verevkin, S. P. Thermodynamic properties of caffeine:  
26 Reconciliation of available experimental data. *J. Chem. Thermodyn.* **2008**, *40*, 1661–1665.

27  
28  
29 (64) De Gusseme, A.; Neves, C.; Willart, J. F.; Rameau, A.; Descamps, M. Ordering and  
30 disordering of molecular solids upon mechanical milling: the case of fananserine. *J. Pharm.*  
31 *Sci.* **2008**, *97*, 5000–5012.  
32  
33  
34  
35  
36  
37  
38  
39  
40  
41  
42  
43  
44  
45  
46  
47  
48  
49  
50  
51  
52  
53  
54  
55  
56  
57  
58  
59  
60

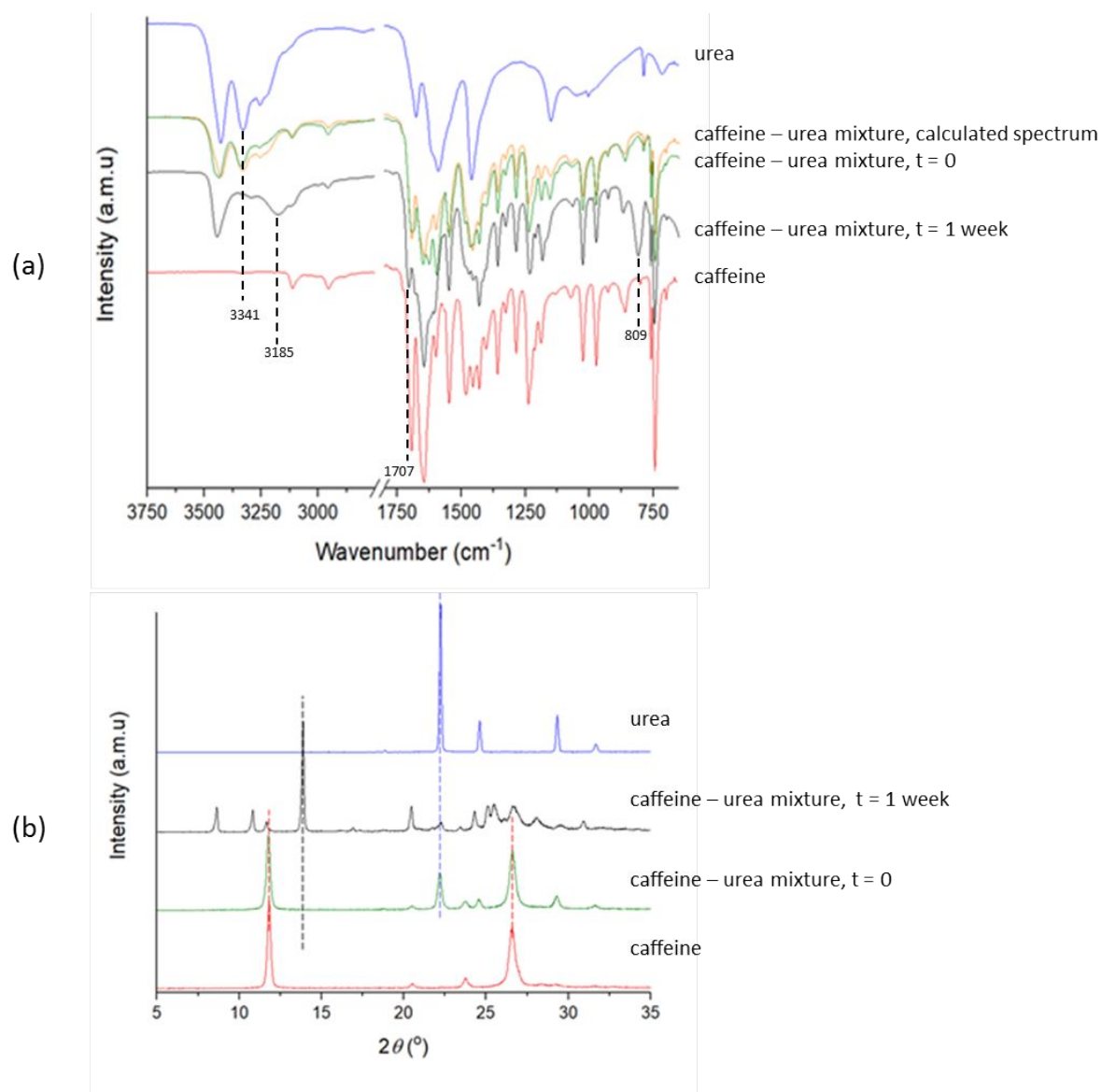


**Figure 1.** (a) IR spectra and (b) PXRD patterns of urea (blue), caffeine (red), a physical 1:1 mixture of urea and caffeine immediately after milling (green), a physical 1:1 mixture of urea and caffeine after milling and storage for one week (black) and the calculated IR spectrum of a physical 1:1 mixture of urea and caffeine (yellow).

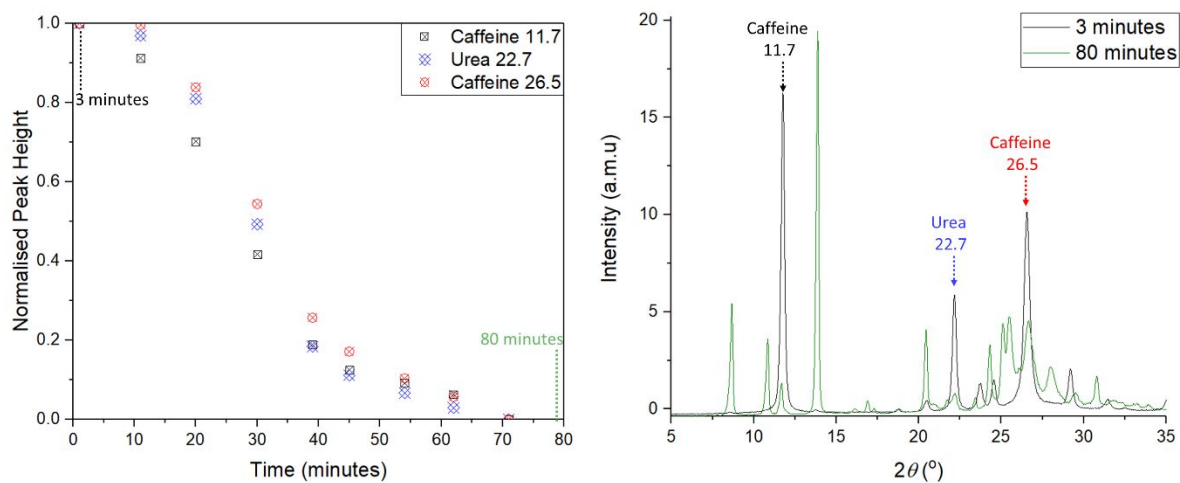


**Figure 2.** Transformation of caffeine and urea to the co-crystal during storage of milled 1:1 mixtures over time using PXRD. (a) Plot of the normalized peak heights of the caffeine peaks at 11.7 and 26.5 ° ( $2\theta$ ) and of the urea peak at 22.7 ° ( $2\theta$ ). (b) PXRD patterns after storage for 3 (black) and 80 (green) min.

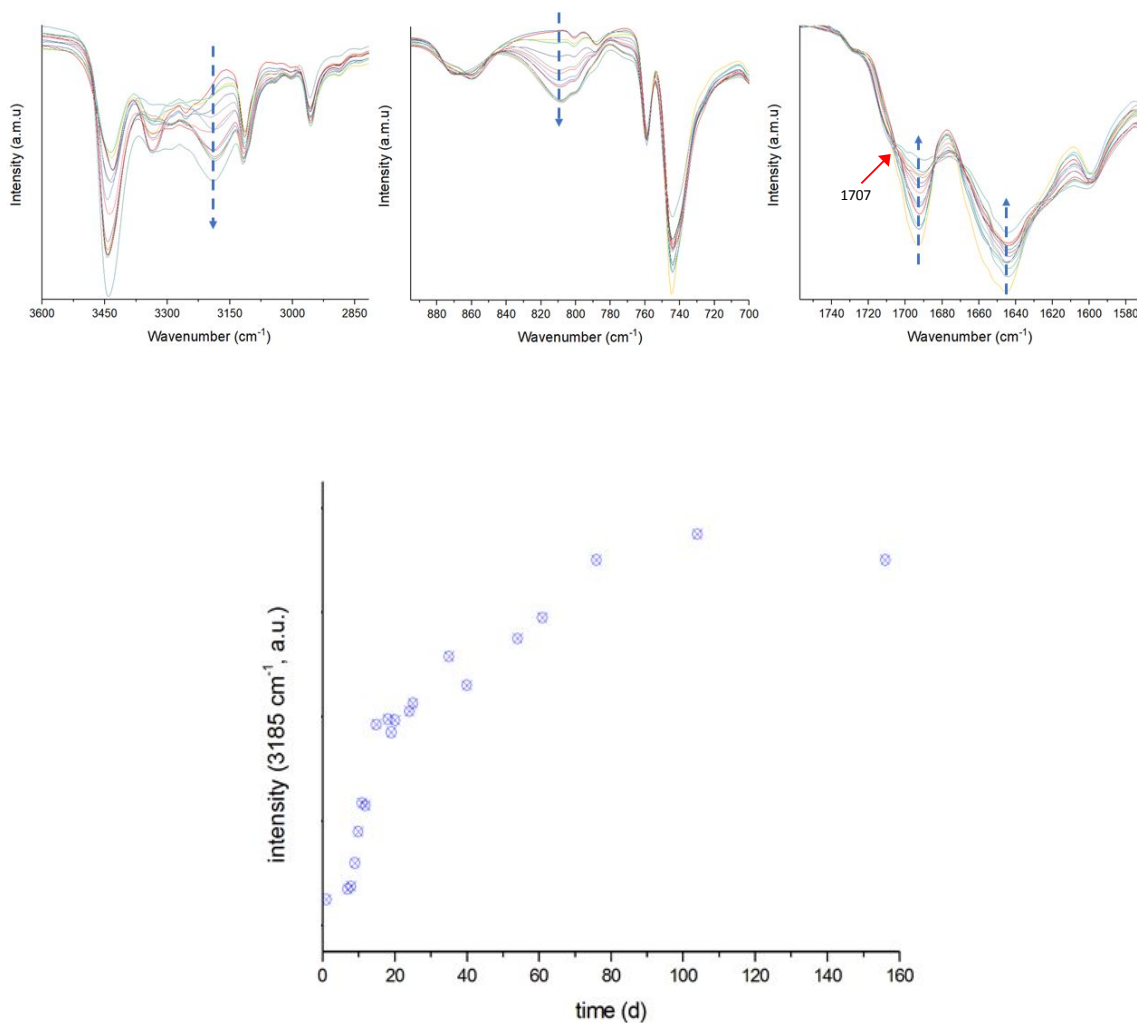


**Figure 3.** Time-dependent changes in the 2850 – 3600 cm<sup>-1</sup>, 700 – 880 cm<sup>-1</sup> and 1580 – 1740 cm<sup>-1</sup> ranges of the IR spectrum of a 1:1 mixture of separately pre-milled caffeine and urea during low energy mixing over 23 weeks (top). Increase of the intensity of the co-crystal peak at 3185 cm<sup>-1</sup> from SNV treated data (bottom).



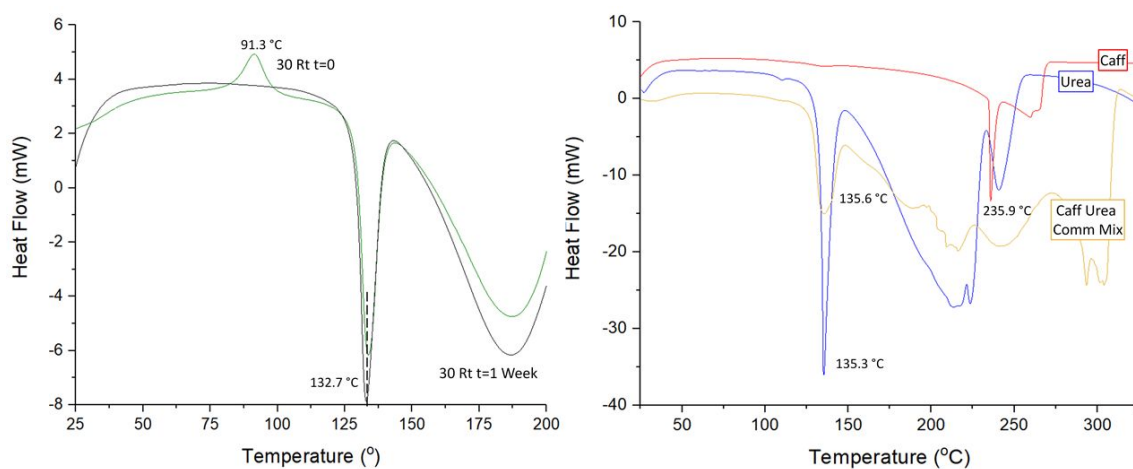


**Figure 4.** DSC plots of samples of caffeine (red), urea (blue), a 1:1 caffeine-urea mixture immediately after milling (green), a 1:1 caffeine-urea mixture after milling and storage for 24 h (black), and a physical mixture of (un-milled) caffeine and urea (yellow).

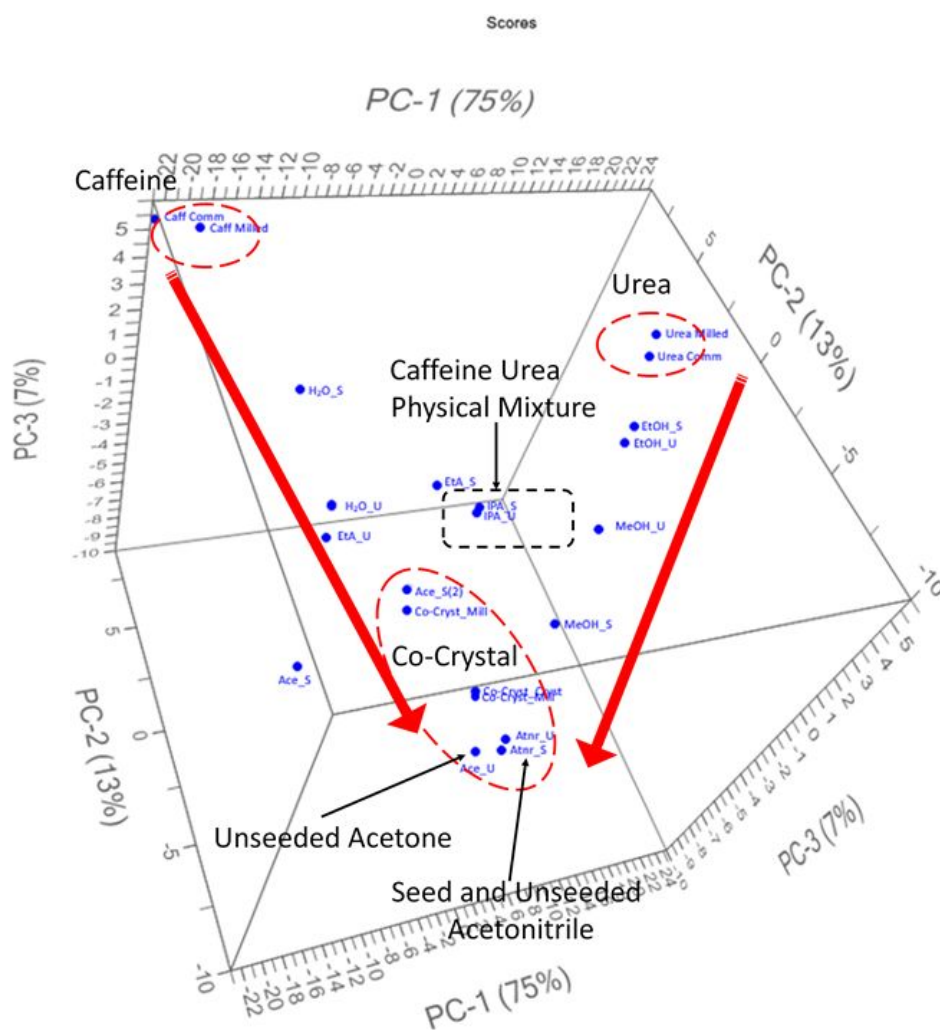


**Figure 5.** PCA scores plot of the IR spectra of caffeine-urea co-crystallization by solvent evaporation.

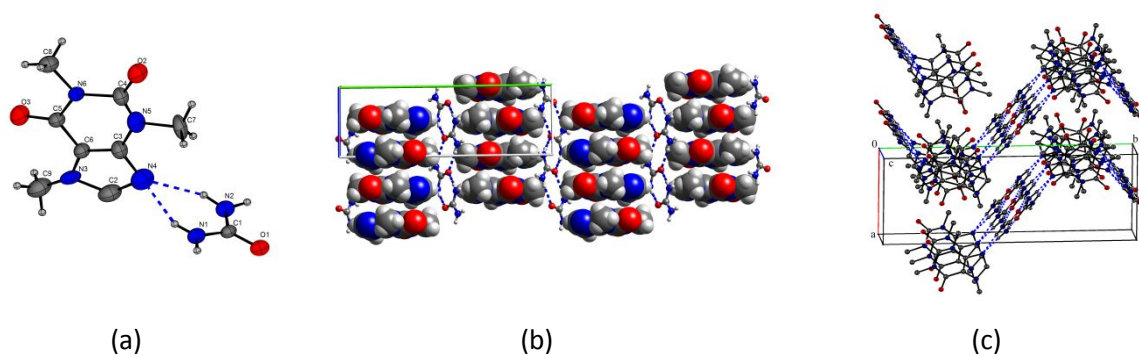


**Figure 6.** (a) Asymmetric unit of the caffeine-urea co-crystal with the principal component of the caffeine disorder shown. (b) Hydrogen bonded urea chains running parallel to *c* with hydrogen bonded caffeine molecules and (c) urea chains and caffeine stacking along the *c* direction (H atoms not involved in H-bonding not drawn for clarity).

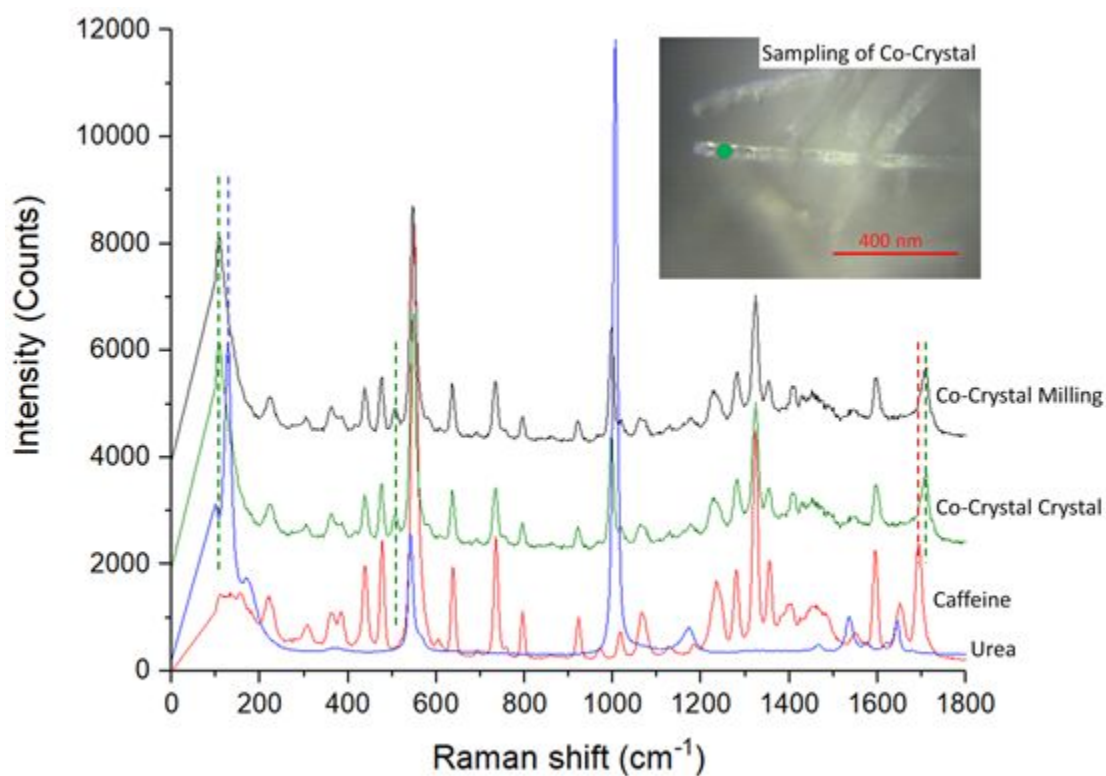


**Figure 7.** Raman microscopy spectrum of a single co-crystal (green), compared to spectra of caffeine (red) and urea (blue), and the spectrum of the co-crystal formed after milling and storage (black).

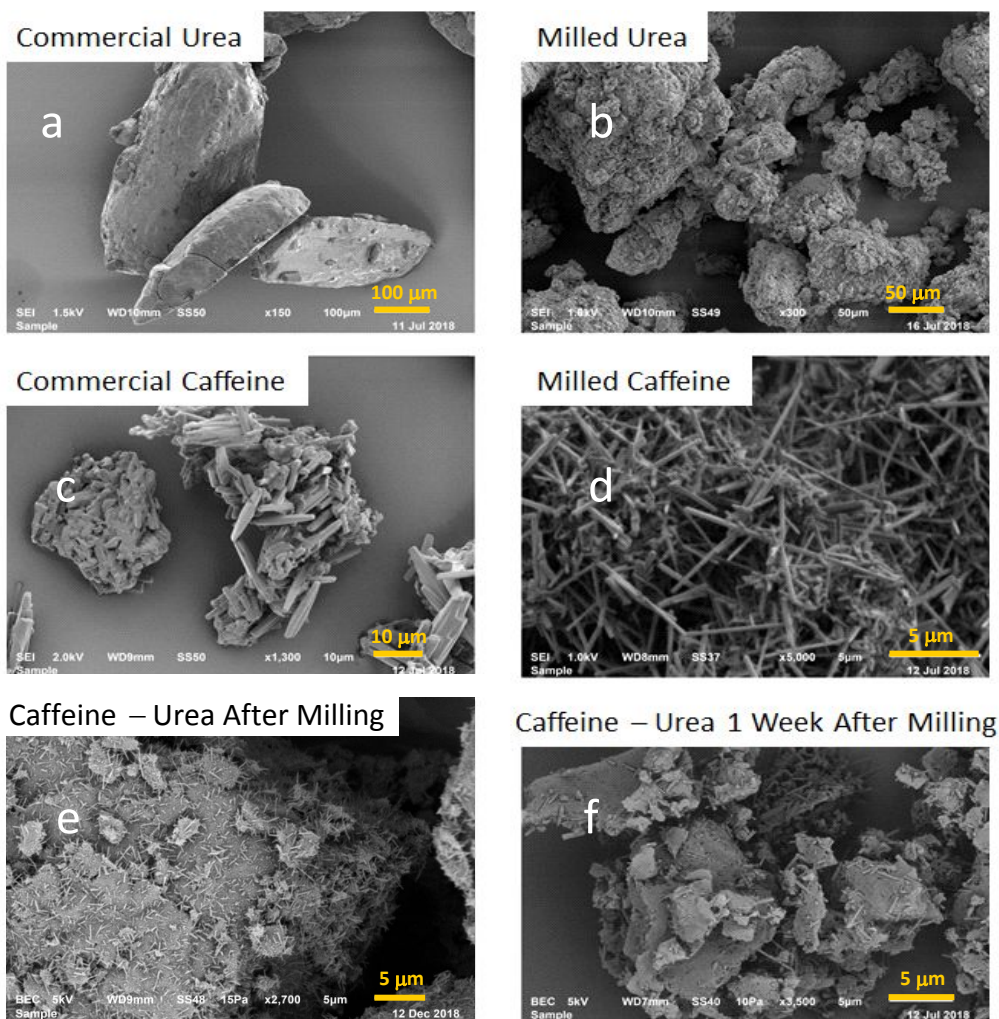


**Figure 8.** SEM images of urea and caffeine before and after milling (a-d) and milled 1:1 mixtures of caffeine and urea directly after milling (e) and after storage for one week at room temperature (f).

**Table 1.** Crystal data of the urea-caffeine cocrystal.

---

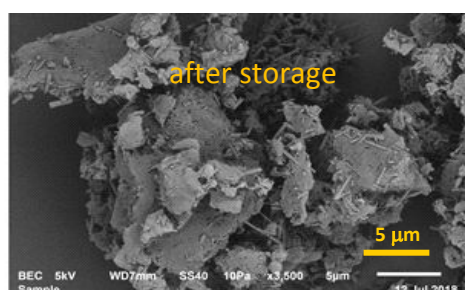
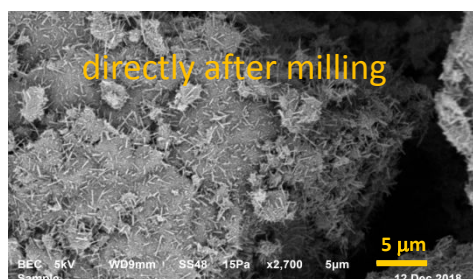
Formula	$C_9H_{13}N_6O_3$
$M_r$	253.25
Crystal colour and habit	colourless block
Crystal size (mm)	$0.50 \times 0.40 \times 0.20$
Crystal system	monoclinic
Space group	$P2_1/c$
Unit cell dimensions	
$a$ [Å]	8.6741(8)
$b$ [Å]	20.421(2)
$c$ [Å]	7.1057(7)
$\beta$ [°]	110.300(10)
$V$ [Å <sup>3</sup> ]	1180.5(2)
$Z$	4
$D_{\text{calc}}$ (g cm <sup>-3</sup> )	1.425
No. measd. reflections	4786
no. unique reflections ( $R_{\text{int}}$ )	2628 (0.0165)
No. obs. reflections	1600
Final $R_1$ , $wR_2$ (obs. refl.)	0.1021, 0.2825
Goodness-of-fit (obs. refl.)	1.094

---

1  
2  
3 **For Table of Contents Use Only**  
4  
5  
6  
7  
8

9 **Spontaneous Solid-State Co-Crystallization of Caffeine and Urea**  
10  
11  
12

13 Pól MacFhionnghaile, Clare M. Crowley, Patrick McArdle,\* and Andrea Erxleben\*  
14  
15  
16  
17  
18  
19  
20  
21  
22



Enhanced inter-particle surface contact in a milled physical mixture of caffeine and urea leads to the spontaneous transformation to the caffeine-urea cocrystal on storage at room temperature and <30 % RH.